Imaging the tarsal plate: A Mini-Review

Alberto Recchioni[1,2]

[1] Academic Unit of Ophthalmology, Institute of Inflammation and Ageing, University of Birmingham, Birmingham and Midland Eye Centre, Birmingham, UK
[2] Optometry & Vision Sciences Group, School of Life & Health Sciences, Aston University, Birmingham, UK

Abstract

Imaging the tarsal plate and the meibomian glands (MG) grants new opportunities for ophthalmic practitioners who work in the field of the ocular surface and dry. The secretory role of MG plays a fundamental part in protecting the moisture covering the surface of the eye by creating an active shield made of meibum (lipid) which prevents tear evaporation and dry eye. The Dry Eye Workshop reports (2007 and 2016) reports that MG dysfunction is the first cause of evaporative dry eye which is also the most common cause of dry eye and ocular surface discomfort. A plethora of instruments for MG observation, diagnosis and follow-up are available in the market. It appears that infrared light technology is the most common in research and clinical practice followed by the in-vivo confocal microscopy and the anterior segment OCT.

The objective of this review is to condense the latest evidence in MG imaging by providing a narrative overview of the most commonly used technologies plus some other aspects which might guide clinicians and researchers in the field of the ocular surface and dry eye.

Keywords: Meibomian glands, Meibomian glands dysfunction, dry eye, diagnostic imaging, meibography

Introduction

"The International Workshop on Meibomian Gland Dysfunction" established the role of meibomian glands (MG) and their dysfunction (MGD) as the most common cause of evaporative dry eye. MGD was defined as *"a chronic, diffuse abnormality of the meibomian glands, commonly characterized by terminal duct obstruction and/or qualitative/quantitative changes in the glandular secretion. This may result in alteration of the tear film, symptoms of eye irritation, clinically apparent inflammation, and ocular surface disease"* (Nelson et al., 2011). Dry eye is a common ophthalmic issue of multifactorial nature where the ocular surface homeostasis is lost resulting in tear film instability, hyperosmolarity and inflammation. Additionally, ocular symptoms such as eye discomfort (e.g., gritty and sore eyes), visual quality decay and light sensitivity may be experienced (Craig et al., 2017).

As cited, one of the most frequent signs of dry eye is the tear film instability that could be related to the weak evaporative resistance of the tear film observed in presence of MGD (Bron et al., 2017). This happens when there is excessive water loss from the exposed ocular surface in the presence of normal lacrimal secretion (Lemp, 2007).

During recent years, clinicians and researchers have been exposed to several techniques for imaging the MG and the area of the palpebral rims. This is particularly important for observation, monitoring and diagnosing the stages of the disease as well as for treating accordingly. In general, the imaging technique is called "meibography" which comprises photographic documentation of the MG using different illuminations and technologies. Historically, meibography started in late 70s when Tapie firstly attempted observing MG structures Tapie (1977). Tapie employed an illumination probe taken from vitreous surgery coupled with a red-light filter which allowed the observation of the MG silhouette through the eyelids. However, the measurement was quite uncomfortable for the patient due to the heat emitted by the light probe and did not provide enough detail for further analysis. Later, Mathers et al. (1994) developed the first real-time video-meibography system where the practitioner could examine MG structures via VHS recordings. However, this technique required several recordings to complete the eyelid margin investigation. Through the years, the main aim of the researchers was to obtain a method for observing MG that could guarantee detailed images with minimal impact on patients' comfort. This was achieved by employing infra-red (IR) illumination as a light source and connecting the probe with a CCD camera sensitive to IR (Arita et al., 2008; Nichols et al., 2005; Pflugfelder et al., 1998). However, meibography development did not stop with IR illumination and newer approaches such as in-vivo confocal microscopy (Kobayashi et al., 2005) and optical coherence tomography have been applied for investigating the eyelids margin (Bizheva et al., 2010).

In this plethora of examination techniques, the objective of this review is to recapitulate the latest available and most commonly used technologies for MG diagnostic imaging.

Materials and methods

A systematic approach was used to perform this review. The review process is detailed in Figure 1 where identification, screening, eligibility, and inclusion steps were assessed. PubMed Search database was searched from the inception. All the records were uploaded to EndNote X9 (Thomson Reuters) to verify any duplicates. Articles assessed for inclusion in this review were identified from 1st January 2016 until 31th September 2021, using individual and combinations of the keywords detailed in the Search Strategy (Annex 1). The period considered (last 5 calendar years) was to follow up the release of the Tear Film Ocular Surface Dry Eye WorkShop 2 (TFOS DEWS II) (Craig et al., 2017) in 2017 which included the latest scientific evidences in the field of dry eye and ocular surface up to 2016.
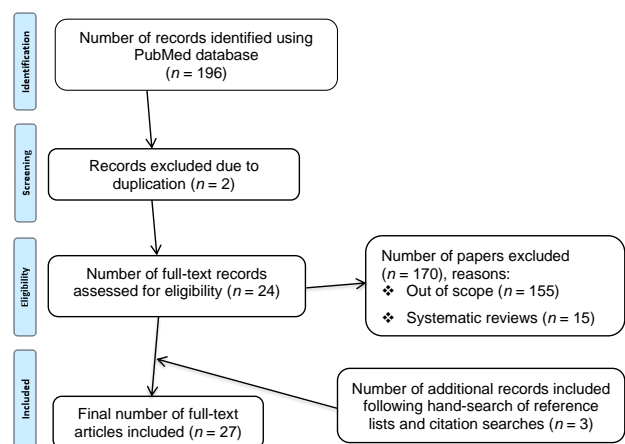

Figure 1: *Flow diagram of the literature search and selection process.*

The search terms included in the search strategy were agreed upon with two different clinicians in the field of dry eyes and MGD. In addition, papers included in the full-text screening process were subjected to a hand search of reference lists which has been conducted using Web of Science (WoS).

Studies were included if they focused on diagnostic techniques used specifically for meibomian glands evaluation and assessment. Additionally, the following eligibility criteria were considered: relevance, full-text access and studies done in humans. Criteria for exclusion were abstract only, lack of relevance, or a non-English language. The search strategy included truncation and phrase searching.

A narrative approach was considered for this review. The focus of this article is to highlight the latest evidence for the most common technologies available for MG and tarsal plate imaging.

Results

In this review the most commonly used MG diagnostic techniques are included: infrared light, IVCM, anterior segment OCT and mixed techniques. These are summarized in Table 1.

Infrared light

Meibography using infrared light (700–1000mm) works by projecting infrared (IR) light onto the everted eyelid which then is recorded via an IR-sensitive camera, removing the need for transillumination of the lid.

For the first time in 2005, Nichols et al. (2005) used a digital video technique for imaging the MG by the means of IR light. The system was composed of a Dolan-Jenner transilluminator coupled with a fibre-optic guide where images from the lower eyelids were acquired with a CCD camera. Later, Yokoi et al. (2007) and Arita et al. (2008) improved the technique by developing non-contact IR meibography which is able to scan the entire area of the MG. Currently, this diagnostic technique is the most common.

One of the most common limitations in considering IR diagnostic imaging for MG evaluation is the need to apply a fast, reliable, and objective grading system. In fact, MG dropout score is usually determined by the clinicians' ability and experience in comparing the scans with the validated grading scales available (e.g., Meiboscore, Meiboscale, etc.).

In their study, Koprowski et al. (2016) described the use of an algorithm for automatically analysing the MG IR images without the need for clinician input. Their algorithm provides a sensitivity of 99.3% (true positive rate) and specificity of 97.5% (false positive rate) allowing the clinician to differentiate between healthy subjects, at-risk subjects, and also differentiate the severity of those patients affected (25%, 50%, 75% of the surface).

However, for those clinicians unable to consider sophisticated algorithms in their clinical practice, there are several ready-to-use diagnostic imaging devices equipped with IR light for detailing the MG structure. One of the most common in the clinical settings is the Keratograph 5M (Oculus, Wetzlar, Germany) which has demonstrated validity in working with dry eye and healthy patients (Abdelfattah et al., 2015). Chen et al. (2017) considered non-contact IR meibography in primary Sjögren's syndrome (SS) patients: the authors reported a higher degree of MGD, glands dropout and eyelid margins irregularities in the autoimmune disease cohort compared to the healthy control group. Also, the study showed a higher percentage of MG atrophy in the lower eyelid in the SS group.

Again, following up on their previous study, Koprowski et al. (2017) improved their algorithm applied to IR meibography evaluation and grading: the results (which don't require operator's intervention) in terms of sensitivity increased at 98% and specificity at 100% with a faster evaluation time of only 0.4 s.

It is relevant to report the results from Wu et al. (2017) who have employed non-contact IR meibography in paediatrics cohorts by comparing children (3 to 11 years old) versus adolescents (12 to 18 years old). The authors reported no relationship in MG dropout with age nor any correlations between the glands, tear and ocular surface functions comparing the cohorts considered. Another important consideration to draw is related to the IR MG scan procedure: Maskin and Testa (2018) reported that caution has to be taken on how the inferior eyelid is pictured. Frequently, an erroneous measure could lead to eyelid distortions and altered vertical gaze directions leading to false conclusions.

Meibography should not be restricted only to a clinical setting equipped with expensive ophthalmic devices: in their study, Osae et al. (2018) reported for the first time results from Africa about MG. They demonstrated that the custom meibographer employed in their study (a cheap IR camera with a +20 D lens) can be the answer for those developing countries where premium technologies might be still limited. In contradiction with previous results (Pult & Nichols, 2012), they found a higher rate of MG loss in the upper lid compared to the lower lid. Additionally, they reported no difference between males and females considered.

Using a non-contact LipiView meibography system (TearScience Inc., Morrisville, N.C.), Park et al. (2018) demonstrated how to track partial or complete loss of the MG in thyroid eye disease (TED) patients. Thanks to the interferometry built-in technology, the LipiView determined the lipid layer thickness of these patients (average, maximum and minimum over a period of 20 s) which is considered an indirect way to observe the MG oil secretion (McCulley & Shine, 2003), and also by providing an analysis of the incomplete blink ratio. The results showed that in this particular cohort of TED patients MG loss was up to 83% and 60% in the upper and lower eyelid, respectively. Although the LLT values were normal and not predictable of higher MGD in TED patients, the incomplete blinking was recorded high as 51%.

Wong et al. (2019) compared two of the most popular MG analysers; the Keratograph 5M and the LipiView II Ocular Surface Interferometer (LVII) (Johnson & Johnson Vision, Jacksonville, FL, USA). While the Keratograph 5M uses a wide-field IR camera, the LVII can obtain MG images from three different sources: dynamic illumination, adaptive transillumination and dual-mode dynamic meibomian imaging. The dynamic illumination aims to reduce the MG glare and backscatter, the adaptive transillumination changes the light intensity to compensate for the eyelid thickness variations between patients. Finally, the dual-mode combines both dynamic and adaptive transillumination to enhance the MG visualization. The authors demonstrated that in their cohort (20 subjects, 40 images in total) despite both devices working with IR illumination, they were not interchangeable in performing MG analysis on the lower eyelid. This lack of agreement might be due to the poorer contrast and to the increased glare of the images.

Shehzad et al. (2019) developed and compared semi-automated software for MG analysis. The authors acquired 52 images from MGD and healthy patients through a CSO Sirius Topographer (CSO, Florence, Italy) which is based on a Placido disk technology with a Scheimpflug camera equipped with IR illumination. They compared the manual method (manually marking of the tarsus borders) versus semi-automated (MATLAB and Image Processing Toolboxes) and found that the first method requires at least a draw of 100 dots to determine MG (time needed 15 ± 3.4 min) versus the semi-automated which requires less than 1 minute. However, both analyses were significantly correlated ($r = 0.95$, $p < 0.001$) and there was "good" to "very good" agreement in grading the results.

Another IR illumination technique with the Scheimpflug rotating camera mounted in the Sirius Topographer: Gulmez Sevim et al. (2020) measured 130 volunteer patients with the

Table 1: *Summary of the technologies discussed in this review.*

Technology	Requirements	Applications	Advantages	Disadvantages
Infrared light (IR light)	IR light and IR-sensitive camera	Meibomian glands and tarsal plates	Quick, easy, and non-invasive	Lack of objective/automatic grading
In-vivo confocal microscopy (IVCM)	Laser scanning device	Ocular surface such as cornea, conjunctiva, meibomian glands, tarsal plates, etc.	Improved contrast and better resolution (1 μm per pixel)	Requires anaesthetic. Some patients might not tolerate the examination (anxious patients, paediatric patients, etc.). Requires training or expert operator
Anterior segment optical coherence tomography (AS-OCT)	Time-domain, spectral-domain, or swept-source indirect interferometry scanning device	Ocular surface such as cornea, conjunctiva, meibomian glands, tarsal plates, etc.	Faster and non-invasive image acquisition (up to 400,000 A-scans/second). Three-dimensional images.	Device cost. Requires training or expert operator. Lack of specific software for MG and tarsal plate analysis
		Other devices		
Meibometer	Photometer device	Tear film components (e.g., lipids)	Non-invasive	Requires a lab-suite for analysis
Red filter system (RFS)	Red filter applied to a digital slit-lamp	Meibomian glands	Non-expensive. Widely available	Level of details. Lower interobserver reliability

Sirius to explore the correlations of MGD severity with the other dry eye metrics such as the Ocular Surface Disease Index (OSDI) questionnaire, fluorescein break-up time and conjunctival straining with Lissamine green. The researchers, considering two clinicians as evaluators, found significant correlations across MGD severity, MG area of loss and all the previous metrics cited. Interestingly, while age ($r = 0.21$, $p = 0.015$) and atrophy ($r = 0.24$, $p = 0.005$) in the lower eyelid were determinants in MGD, gender was not (p range 0.66–0.95). This study remarks that MGA loss percentage measurements using a Sirius Topographer are highly repeatable (ICC values 0.994, 95% CI: 0.992–0.995, for reader 1 and 0.988, 95% CI: 0.982–0.992, for reader 2).

Yin and Gong (2019) focused their research work on a new parameter for MG analysis: MG vagueness. In fact, some patients might present a vague and difficult to identify MG structure in both upper and lower eyelids. The newly defined index was found clinically significant with the area under the curve (AUC) over 70 with a specificity of 83% (n = 47 MGD patients). Also, MG vagueness was found significantly correlated with MGD severity at all levels, MG acinar shortest diameter ($r = -0.278$, $p = 0.017$), OSDI questionnaire score ($r = -0.3271$, $p = 0.001$) and tear break-up time ($r = 0.405$, $p = < 0.001$). Cieżar and Pochylski (2020) applied the Fourier image transformation to the MG analysis. In particular, the authors proposed two new metrics such as the "mean gland frequency" (i.e., number of glands per unit length) and "anisotropy of gland periodicity" to study the whole eyelid area. When images from healthy and unhealthy subjects were considered, nearly 100% accuracy (n = 146 images) was achieved by the Fourier image transformation. However, the algorithm showed a limit when evaluating the "intermediate" category of MG severity: this can be explained because of the overlap between the two main categories of images (healthy and unhealthy). In fact, the categorisation of the ground-truth images on which the algorithm is based was initially decided by the expert (human-related uncertainty).

J. S. Lee et al. (2020) described the clinical accuracy of a relatively new device called Antares (Lumenis, Australia) which combines the functionality of a non-contact Placido disk topographer with an IR camera for MG imaging with the LipiView system described above. With a cohort of 33 Korean patients, the authors noted that the IR images acquired from both devices were correlated ($r = 0.446$, $p = 0.009$). They also reported that the Antares images were poorer in quality compared with the LipiView due to lack of contrast, lighter background, and greater

reflections. The MG tortuosity parameter explored by Lin et al. (2020) in their work, highlights how MG imaging and analysis has become increasingly detailed over the past years. Based on their findings in 32 and 28 MG obstructive and healthy patients respectively, they reported that MG tortuosity of the upper eyelid can be considered to diagnose MGD due to obstruction. Sensitivity and specificity were 90% and 100% for the average tortuosity of all MGs and 80% and 100% for the average tortuosity of the central eight MGs, respectively. Therefore, we can assume from Lin et al.'s results, that MG tortuosity should be considered as a reliable sign to monitor MGD, but further studies with greater sample sizes are required.

Maskin and Alluri (2020) showed by IR illumination, the ability to locate and internally cannulate MG: the researchers progressed further by assessing the intraductal space, which can open an interesting scenario on the treatments for MG rehabilitation. In fact, the results showed that signs and symptoms such as lid tenderness and lid functionality (meibum secretion and the number of expressible glands) were improved after intraductal probing. In their study, they used a specific set of probes tested for MG ducts whose diameters were less than 110 microns and lengths were 1, 2 and 4 mm. The temporary insertion of these probes also aims to reduce MG tortuosity by straightening the ducts.

Based on 120 healthy subjects MG IR images obtained with a Keratograph 5M, García-Marqués et al. (2021) developed a new algorithm using MATLAB to objectively measure MG visibility, which should be differentiated from measuring MG loss or any previous MG metrics studied. Their outcomes showed that MG visibility could anticipate MGD which affects lipid secretion and composition. Furthermore, the algorithm is capable of classifying patients according to their MGD severity: within-subject standard deviation (Sw), coefficient of variation (CoV), and repeatability coefficient (CoR) indicated "good" repeatability even if the IR scans were manually acquired by an experienced operator. Finally, higher MG visibility might be related to a better MG status in terms of functionality, while lower MG visibility might relate to a higher MG dropout.

Despite the majority of studies included in this review being based on adult cohorts, IR illumination can be helpful also in the paediatric population. In their study, Kara and Dereli Can (2021) considered anterior segment parameters acquired with a corneal topographer equipped with IR illumination in 37 children/adolescents (age range 5 to 17) affected with isolated

growth hormone deficiency (GHD). Their findings revealed that the GHD group had up to 79.4% of MG loss despite having a similar MG morphology distortion as the healthy group ($n=40$).

In-vivo confocal microscopy (IVCM)

IVCM is an invasive technique to obtain detailed high-resolution images of the human ocular surface (cornea, conjunctiva, tear film and annexes). IVCM can be divided into tandem, slit, and laser scanning devices (De Silva et al., 2017). However, the most common IVCM devices are based on the laser scanning principle which is unharmful to the eye (red wavelength 670 nm) and yields optimal scans in terms of depth of focus (800–fold magnification), improved contrast and better resolution (1 μm per pixel). IVCM enables analysis of cell layers, which might show abnormalities and the presence, type and location of infections and inflammation. This provides vital additional information for patients both in the acute and chronic stages of the disease process. IVCM applications range from early detection of microbial keratitis (Hassan et al., 2019), reduction in corneal after ophthalmic surgery (Recchioni et al., 2020), assessment of rare genetic diseases (Leonardi et al., 2020), dry eye screening and diagnosis (Hwang et al., 2021), etc. In the context of MG imaging, IVCM can observe fine details of the MG anatomical structure, which might suggest any abnormalities leading to MGD. Zhao et al. (2016) explored the relationship between MG structure and dry eye metrics in a cohort of dry eye patients ($n=60$): they studied several new MG metrics such as MG acinar unit density (MGAUD), MG acinar unit area (MGAUA), MG acinar unit longest diameter (MGALD) and MG acinar unit shortest diameter (MGASD). Their results showed that the patients with the highest symptomatology scores (OSDI and Salisbury Eye Evaluation Questionnaire (SEEQ)) were also those with the most severe degree of fibrosis and atrophy of MGs. Additionally, all the observed MG metrics between mild and severe dry eye patients exhibit changes in cell size and density, leading to MGD. Randon et al. (2019) defined a four type MG classification based on IVCM imaging: type 0 = no MGD, type 1 = obstructive disease, type 2 = inflammatory disease and type 3 = fibrosis state. In order to define these four types, the authors considered meibum (MG secretion) reflectivity, intraepithelial/interglandular inflammation, and glandular fibrosis which showed mild correlations with the dry eye metrics such as tear osmolarity, ocular staining score (Oxford grading scheme), tear break-up time, and Schirmer test (n = 101 dry eyes and 15 healthy eyes). Finally, an initial IVCM mild type of MG classification (type 1 obstructive disease) could suggest early MG treatment (e.g., warm compress and massage, eyelid hygiene, etc.) which could avoid the worsening of patient dry eye signs and symptoms.

Controversially, S. Zhou and Robertson (2018) focused their work on confirming if the MG structures observed in previous investigations Matsumoto et al. (2008) were MG or something else. In their methods, a comparison between in-vivo and in-situ by using immunofluorescence was adopted to define that those structures believed to be MG were, in reality, rete ridges in the dermal-epidermal junction of the eyelids (e.g., epithelial extensions). Nevertheless, using quantitative image analysis (MetaMorph software), the researchers also calculated the morphologic profile of these rete ridges, although without any clarification of whether these were in related to MGD.

Maruoka et al. (2020) considered 137 IVCM images from 137 obstructive MG individuals to evaluate the performance of image processing using deep learning models in MGD diagnosis. The deep convolutional neural network (DNN) developed was able to distinguish with high sensitivity, specificity, and AUC healthy versus dysfunctional MG subjects. This automatic DNN classification poses a new frontier in ophthalmology imaging

in MG because artificial intelligence will allow nearly the same classification accuracy as an expert examiner with less buy in human and economic resources.

Finally, the work by N. Zhou et al. (2020) could help clinicians to define a feasible protocol for those interested in working with IVCM in MG. The researchers suggested that the evaluation of the eyelid margin should include at least five non-overlapping single frames of rete ridges area and at least three MG openings at 20 μm depth intervals between 30 and 130 μm. However, as remarked in this study, IVCM imaging of MG should be carefully evaluated as evidence confirms that only structures such as rete ridges, MG openings and lid wiper region can be observed (Maruoka et al., 2020). Further studies are needed to determine which of the eyelid structures observed with IVCM imaging are most sensitive to MGD.

Anterior segment optical coherence tomography

Anterior segment optical coherence tomography (AS-OCT) is a non-contact imaging method that provides detailed cross-sectional images of biological tissues. It works with a similar principle as ultrasound imaging and can be used for defining structures such as ocular surface, anterior chamber, crystalline lens, etc(**empty citation**)Jiao2019. Several types of AS-OCT technology are available and can be classified into time-domain, spectral-domain, and swept-source. They are all based on the same principle of indirect interferometry, in which a beam of light is directed into the retina. The back-scattered light distance is measured with a detector, which is then compared to a reference beam of known length to calculate the echo time delay of light. With time-domain AS-OCT, the echo time delays are measured one at a time while spectral-domain and swept-source AS-OCTs have a fixed-reference arm to generate an interference pattern of the reflected light. By using Fourier transformation, all these echo measurements can be obtained simultaneously and this has increased the image acquisition speed of these devices to up to 400,000 A-scans/second (Potsaid et al., 2010)). During recent years, modern AS-OCT technologies such as spectral-domain and swept-source have been adopted for examining the ocular surface and the tear film in dry eye disease (Venkateswaran et al., 2018). The newest AS-OCT swept-source light employs 1310 nm IR light source and makes it possible to reconstruct the three-dimensional images of the anterior segment of the eye more accurately by providing useful information before and after corneal and lens surgeries or treatment, and in determining the hereditary or infective aetiology of corneal pathologies.

Napoli et al. (2016) used a spectral-domain OCT (840 nm, 27,000 axial scans/s, 5 μm axial resolution) to image both the upper and lower eyelids of 61 and 75 obstructive MGD and healthy patients, respectively. Essentially, their aims were to describe this technology applied to the MG imaging and to demonstrate the feasibility of using the built-in software to enhance OCT scans. More importantly, the authors were interested in reducing patients' discomfort by avoiding invasive techniques (contact meibography), and hospital costs by considering a technology already available for ophthalmic imaging of the posterior segment (Cirrus HD-OCT 4000, Carl ZeissMeditec Inc., California, USA). Their findings revealed substantial agreement with standard meibography, introducing new metrics in MG assessment such as the segmentation (MG appear divided into pieces in their row) and entanglement (MG exhibit a tangled pattern in their row). While segmentation was observed in patients with lower dropout grades (early screening of MGD), entanglement was more present in the atrophic process related to higher dropout grades (follow-up of MGD).

In their cross-sectional study, Yoo et al. (2017) considered a

custom AS-OCT with a long wavelength (1310nm) and high-speed data processing (50 kHz) to obtain 3D reconstruction images of MG in 275 cases of MGD. By comparing AS-OCT scans with IR light scans, the researchers revealed a 3-scale classification system based on MG acini and ducts (Group 1 = constricted acini, Group 2 = atrophic acini, Group 3 = no acini), which might help clinicians to further assess and treat MG patients.

Wang et al. (2020) proposed a new application of AS-OCT for patients in the early stages of MGD or completely asymptomatic: in their research, they measured the lower lid margin thickness (LLMT) from the posterior lash line to the Marx's line and compared the results with a vernier micrometre (e.g., ruler). The reason behind this methodology is that thickening of the lid margin is a common feature of MGD (Knop et al., 2011), but also of blepharitis, lid wiper epitheliopathy, etc. The results found that AS-OCT is a reliable technique (ICC = 0.83) compared to vernier micrometre for rapid and non-invasive in-vivo imaging of fine structures of the eye such as the eyelid margin.

Other devices

An indirect measurement of the current MG functionality is the photometric assessment of optical density done over a sample of lipid layer called meibometry. This measurement can be done by collecting a small sample from the lid margin with a device called meibometer and then observing through a photometer (Chew et al., 1993). The meibometer basic principle is that the light transmission is increased in presence of oil (lipid). García-Resúa et al. (2017) employed a Meibometer MB550 (Courage-Khazaka electronic GmbH, Cologne, Germany) to assess the ability to distinguish between healthy and abnormal subjects classified with two of the most common dry eye questionnaires (OSDI and McMonnies). Additionally, the authors ascertained the relationship between meibometry and break-up time (BUT) and maximum blink interval (MBI). Symptomatic subjects showed lower meibometer units (MU) than the asymptomatic with significant correlations between MU, BUT and MBI. However, further work is required, such as higher symptomatic and wider age range samples.

Another interesting approach is from S. M. Lee et al. (2019) where a red filter system (RFS) applied to a digital slit-lamp was used to obtain images from 125 eyes (upper and lower eyelids) which were then compared with the gold-standard IR meibography. All the red filter images were initially converted into black and white and adjusted for contrast/brightness before being randomly presented to two independent evaluators together with the IR scans. From their results, it is possible to ascertain that MG dropout measured with an RFS had substantial agreement (weighted $K = 0.676$, 95% CI = 0.594–0.759) with IR illumination technology. Therefore, it can be assumed that MG dropout can be considered even in absence of the gold standard IR illumination technology although with a potential limitation observed within a relatively lower inter-observer reliability.

Conclusion

In this mini-review, the latest available and most common technologies for MG diagnostic imaging were recapitulated. Relevant principles for tarsal plate imaging were discussed under four main domains for the ease of the readers. Meibomian gland and tarsal plate imaging are a valuable support for diagnosis, treatment, and follow-up of one of the most acknowledged causes of dry eye disease, the meibomian gland dysfunction.

In recent years, several new technologies have been made available for clinicians and researchers in the field of ocular surface- and dry eye disease, with the non-infrared illumination technology being one of the most common.

At this moment, the availability of devices able to image the MGs and the tarsal plates differs from setting to setting (public health vs. private sector), from clinician to clinician (ophthalmologist vs. optometrist/optician) and from country to country. It appears that the future development of less expensive devices (e.g., cheap and reliable IR cameras) might help to close the gap and offer these imaging technologies to a wider audit of dry eye patients.

On the one hand, it is true that meibography can provide images of great detail for the clinicians, but on the other hand there is still a lack of a unified method of grading and most clinicians develop and use their own grading system. For example, while classification and grading scales for MG atrophy and orifices secretion are already available thanks to the works of Arita et al. (2008) and Pult and Nichols (2012), there are still gaps in the literature about grading dilation and distortion/tortuosity of the gland.

Finally, larger population studies with wider age, gender and risk factors categories should be undertaken to reveal the efficacy of these newer devices for both clinicians', researchers' and patients' benefit.

References

Abdelfattah, N., Dastiridou, N., Sadda, S., & Lee, O. (2015). Noninvasive imaging of tear film dynamics in eyes with ocular surface disease. *Cornea, 34*, S48–52.

Arita, R., Itoh, K., Inoue, K., & Amano, S. (2008). Noncontact infrared meibography to document age-related changes of the meibomian glands in a normal population. *Ophthalmology, 115*, 911–915.

Bizheva, K., Lee, P., Sorbara, L., Hutchings, N., & Simpson, T. (2010). In vivo volumetric imaging of the human upper eyelid with ultrahigh-resolution optical coherence tomography. *Journal of Biomedical Optics, 15*.

Bron, A., De Paiva, C., Chauhan, S., Bonini, S., Gabison, E., Jain, S., Knop, E., Markoulli, M., Ogawa, Y., Perez, V., Uchino, Y., Yokoi, N., Zoukhri, D., & Sullivan, D. (2017). TFOS DEWS II pathophysiology report. *Ocular Surface, 15*, 438–510.

Chen, X., Utheim Ø, A., Xiao, J., Adil, M. Y., Stojanovic, A., Tashbayev, B., Jensen, J. L., & Utheim, T. P. (2017). Meibomian gland features in a Norwegian cohort of patients with primary Sjögren's syndrome. *PLoS One, 12*(9), e0184284. https://doi.org/10.1371/journal.pone.0184284

Chew, C. K., Jansweijer, C., Tiffany, J. M., Dikstein, S., & Bron, A. J. (1993). An instrument for quantifying meibomian lipid on the lid margin: The Meibometer. *Current Eye Research, 12*, 247–254.

Ciężar, K., & Pochylski, M. (2020). 2D Fourier transform for global analysis and classification of meibomian gland images. *The Ocular Surface, 18*(4), 865–870. https://doi.org/10.1016/j.jtos.2020.09.005

Craig, J., Nichols, K., Akpek, E., Caffery, B., Dua, H., Joo, C., Liu, Z., Nelson, J., Nichols, J., Tsubota, K., & Stapleton, F. (2017). TFOS DEWS II definition and classification report. *Ocular Surface, 15*, 276–283.

De Silva, M. E. H., Zhang, A. C., Karahalios, A., Chinnery, H. R., & Downie, L. E. (2017). Laser scanning in vivo confocal microscopy (IVCM) for evaluating human corneal sub-basal nerve plexus parameters: Protocol for a systematic review. *BMJ Open, 7*.

García-Marqués, J. V., García-Lázaro, S., Martínez-Albert, N., & Cervinño, A. (2021). Meibomian glands visibility assessment through a new quantitative method. *Graefe's Archive for Clinical and Experimental Ophthalmology*, 259, 1323–1331.

García-Resúa, C., Pena-Verdeal, H., Giráldez, M. J., & Yebra-Pimentel, E. (2017). Clinical relationship of meibometry with ocular symptoms and tear film stability. *Contact Lens and Anterior Eye*, 40(6), 408–416. https://doi.org/10.1016/j.clae.2017.07.003

Gulmez Sevim, D., Gumus, K., & Unlu, M. (2020). Reliable, noncontact imaging tool for the evaluation of meibomian gland function: Sirius meibography. *Eye Contact Lens*, 46 Suppl 2, S135–s140. https://doi.org/10.1097/icl.0000000000000651

Hassan, A., F.and Bhatti, Desai, R., & Barua, A. (2019). Analysis from a year of increased cases of Acanthamoeba Keratitis in a large teaching hospital in the UK. *Contact Lens and Anterior Eye*, 42, 506–511.

Hwang, J., Dermer, H., & Galor, A. (2021). Can in vivo confocal microscopy differentiate between sub-types of dry eye disease? a review. *Clinical & Experimental Ophthalmology*, 49, 373–387.

Kara, Ö., & Dereli Can, G. (2021). Topographic and specular microscopic evaluation of cornea and meibomian gland morphology in children with isolated growth hormone deficiency. *International Ophthalmology*, 41(8), 2827–2835. https://doi.org/10.1007/s10792-021-01839-5

Knop, E., Knop, N., Millar, T., Obata, H., & Sullivan, D. (2011). The International Workshop on Meibomian Gland Dysfunction: Report of the Subcommittee on Anatomy, Physiology, and Pathophysiology of the Meibomian Gland. *Investigative Ophthalmology and Visual Science*, 52, 1938–1978.

Kobayashi, A., Yoshita, T., & Sugiyama, K. (2005). In vivo findings of the bulbar/palpebral conjunctiva and presumed meibomian glands by laser scanning confocal microscopy. *Cornea*, 24, 985–988.

Koprowski, R., Tian, L., & Olczyk, P. (2017). A clinical utility assessment of the automatic measurement method of the quality of meibomian glands. *BioMedical Engineering OnLine*, 16(1), 82. https://doi.org/10.1186/s12938-017-0373-4

Koprowski, R., Wilczyński, S., Olczyk, P., Nowińska, A., Węglarz, B., & Wylęgała, E. (2016). A quantitative method for assessing the quality of meibomian glands. *Computers in Biology and Medicine*, 75, 130–8. https://doi.org/10.1016/j.compbiomed.2016.06.001

Lee, J. S., Jun, I., Kim, E. K., Seo, K. Y., & Kim, T. I. (2020). Clinical accuracy of an advanced corneal topographer with tear-film analysis in functional and structural evaluation of dry eye disease. *Seminars in Ophthalmology*, 35(2), 134–140. https://doi.org/10.1080/08820538.2020.1755321

Lee, S. M., Park, I., Goo, Y. H., Choi, D., Shin, M. C., Kim, E. C., Alkwikbi, H. F., Kim, M. S., & Hwang, H. S. (2019). Validation of alternative methods for detecting meibomian gland dropout without an infrared light system: Red filter for simple and effective meibography. *Cornea*, 38(5), 574–580. https://doi.org/10.1097/ico.0000000000001892

Lemp, M. (2007). Methodologies to diagnose and monitor dry eye disease: Report of the Diagnostic Methodology Subcommittee of the International Dry Eye Work-Shop (2007). *Ocular Surface*, 5, 108–152.

Leonardi, A., Carrao, G., Mudugno, R. L., Rossomando, V., Scalora, T., Lazzarini, D., & Calò, L. (2020). Cornea verticillata in Fabry disease: A comparative study between slit-lamp examination and in vivo corneal confocal microscopy. *British Journal of Ophthalmology*, 104, 718–722.

Lin, X., Fu, Y., Li, L., Chen, C., Chen, X., Mao, Y., Lian, H., Yang, W., & Dai, Q. (2020). A novel quantitative index of meibomian gland dysfunction, the meibomian gland tortuosity. *Translational Vision Science and Technology*, 9(9), 34. https://doi.org/10.1167/tvst.9.9.34

Maruoka, S., Tabuchi, H., Nagasato, D., Masumoto, H., Chikama, T., Kawai, A., Oishi, N., Maruyama, T., Kato, Y., Hayashi, T., & Katakami, C. (2020). Deep neural network-based method for detecting obstructive meibomian gland dysfunction with in vivo laser confocal microscopy. *Cornea*, 39(6), 720–725. https://doi.org/10.1097/ico.0000000000002279

Maskin, S. L., & Alluri, S. (2020). Meibography guided intraductal meibomian gland probing using real-time infrared video feed. *British Journal of Ophthalmology*, 104(12), 1676–1682. https://doi.org/10.1136/bjophthalmol-2019-315384

Maskin, S. L., & Testa, W. R. (2018). Infrared video meibography of lower lid meibomian glands shows easily distorted glands: Implications for longitudinal assessment of atrophy or growth using lower lid meibography. *Cornea*, 37(10), 1279–1286. https://doi.org/10.1097/ico.0000000000001710

Mathers, W. D., Daley, T., & Verdick, R. (1994). Video imaging of the meibomian gland. *Archives of Ophthalmology*, 112, 448–449.

Matsumoto, Y., Sato, E. A., Ibrahim, O. M., Dogru, M., & Tsubota, K. (2008). The application of in vivo laser confocal microscopy to the diagnosis and evaluation of meibomian gland dysfunction. *Molecular Vision*, 14, 1263–1271.

McCulley, J. P., & Shine, W. E. (2003). Meibomian gland function and the tear lipid layer. *Ocular Surface*, 1, 97–106.

Napoli, P. E., Coronella, F., Satta, G. M., Iovino, C., Sanna, R., & Fossarello, M. (2016). A simple novel technique of infrared meibography by means of spectral-domain optical coherence tomography: A cross-sectional clinical study. *PLoS One*, 11(10), e0165558. https://doi.org/10.1371/journal.pone.0165558

Nelson, J. D., Shimazaki, J., Benitez-Del-Castillo, J. M., Craig, J. P., McCulley, J. P., Den, S., & Foulks, G. N. (2011). The international workshop on meibomian gland dysfunction: Report of the definition and classification subcommittee. *Investigative Ophthalmology & Visual Science*, 52, 1930–1937.

Nichols, J. J., Bernsten, D. A., Mitchel, G. L., & Nichols, K. K. (2005). An assessment of grading scales for meibography images. *Cornea*, 24, 382–388.

Osae, E. A., Ablorddepey, R. K., Horstmann, J., Kumah, D. B., & Steven, P. (2018). Assessment of meibomian glands using a custom-made meibographer in dry eye patients in Ghana. *BMC Ophthalmology*, 18(1), 201. https://doi.org/10.1186/s12886-018-0869-0

Park, J., Kim, J., Lee, H., Park, M., & Baek, S. (2018). Functional and structural evaluation of the meibomian gland using a LipiView interferometer in thyroid eye disease. *Canadian Journal of Ophthalmology*, 53(4), 373–379. https://doi.org/10.1016/j.jcjo.2017.11.006

Pflugfelder, S. C., Tseng, S. C., Sanabria, O., Kell, H., Garcia, C. G., Felix, C., Feuer, W., & Reis, B. L. (1998). Evaluation of subjective assessments and objective diagnostic tests for diagnosing tear-film disorders known to cause ocular irritation. *Cornea*, 17, 38–56.

Potsaid, B., Baumann, B., Huang, D., Barry, S., Cable, A. E., Schuman, J. S., Duker, J. S., & Fujimoto, J. G. (2010). Ultrahigh speed 1050nm swept source/Fourier domain OCT retinal and anterior segment imaging at 100,000 to 400,000 axial scans per second. *Optics Express*, 18, 20029–20048.

Pult, H., & Nichols, J. J. (2012). A review of meibography. *Optometry and Vision Science*, 89, E760–9.

Randon, M., Aragno, V., Abbas, R., Liang, H., Labbé, A., & Baudouin, C. (2019). In vivo confocal microscopy classification in the diagnosis of meibomian gland dysfunction. *Eye (Lond)*, 33(5), 754–760. https://doi.org/10.1038/s41433-018-0307-9

Recchioni, A., Siso-Fuertes, I., Hartwig, A., Hamid, A., Shortt, A. J., Morris, R., Vaswani, S., Dermott, J., Cervine, A., Wolffsohn, J. S., & O'Donnel, C. (2020). Short-term impact of FS-LASIK and SMILE on dry eye metrics and corneal nerve morphology. *Cornea*.

Shehzad, D., Gorcuyeva, S., Dag, T., & Bozkurt, B. (2019). Novel application software for the semi-automated analysis of infrared meibography images. *Cornea*, 38(11), 1456–1464. https://doi.org/10.1097/ico.0000000000002110

Tapie, R. (1977). *Etude biomicroscopique des glandes de meibomius*.

Venkateswaran, N., Galor, A., Wang, J., & Karp, C. L. (2018). Optical coherence tomography for ocular surface and corneal diseases: A review. *Eye and Vision*, 5.

Wang, D. H., Yao, J., & Liu, X. Q. (2020). Comparison of two measurements for the lower lid margin thickness: Vernier micrometer and anterior segment optical coherence tomography. *International Ophthalmology*, 40(12), 3223–3232. https://doi.org/10.1007/s10792-020-01505-2

Wong, S., Srinivasan, S., Murphy, P. J., & Jones, L. (2019). Comparison of meibomian gland dropout using two infrared imaging devices. *Contact Lens and Anterior Eye*, 42(3), 311–317. https://doi.org/10.1016/j.clae.2018.10.014

Wu, Y., Li, H., Tang, Y., & Yan, X. (2017). Morphological evaluation of meibomian glands in children and adolescents using noncontact infrared meibography. *Journal of Pediatric Ophthalmology & Strabismus*, 54(2), 78–83. https://doi.org/10.3928/01913913-20160929-03

Yin, Y., & Gong, L. (2019). The quantitative measuring method of meibomian gland vagueness and diagnostic efficacy of meibomian gland index combination. *Acta Ophthalmologica*, 97(3), e403–e409. https://doi.org/10.1111/aos.14052

Yokoi, N., Komoro, A., Yamada, H., Maruyama, K., & Kinoshita, S. (2007). A newly developed video-meibography system featuring a newly designed probe. *Japanese Joural of Ophthalmology*, 51, 53–56.

Yoo, Y. S., Na, K. S., Byun, Y. S., Shin, J. G., Lee, B. H., Yoon, G., Eom, T. J., & Joo, C. K. (2017). Examination of gland dropout detected on infrared meibography by using optical coherence tomography meibography. *The Ocular Surface*, 15(1), 130–138.e1. https://doi.org/10.1016/j.jtos.2016.10.001

Zhao, H., Chen, J. Y., Wang, Y. Q., Lin, Z. R., & Wang, S. (2016). In vivo confocal microscopy evaluation of meibomian gland dysfunction in dry eye patients with different symptoms. *Chinese Medical Journal*, 129(21), 2617–2622. https://doi.org/10.4103/0366-6999.192782

Zhou, N., Edwards, K., Colorado, L. H., & Schmid, K. L. (2020). Development of feasible methods to image the eyelid margin using in vivo confocal microscopy. *Cornea*, 39(10), 1325–1333. https://doi.org/10.1097/ico.0000000000002347

Zhou, S., & Robertson, D. M. (2018). Wide-field in vivo confocal microscopy of meibomian gland acini and rete ridges in the eyelid margin. *Investigative Ophthalmology & Visual Science*, 59(10), 4249–4257. https://doi.org/10.1167/iovs.18-24497

Avbildning av tarsalplaten: en oversiktsartikkel

Sammendrag

Avbildning av tarsalplaten og de meibomiske kjertlene (MG) gir nye muligheter for optikere og øyeleger som arbeider med fremre segment og tørre øyne. Den sekretoriske rollen til MG spiller en grunnleggende rolle i å beskytte tårefilmen ved å skape et aktivt skjold av meibum (lipid) som forhindrer tårefordampning og dermed tørre øyne. Dry Eye Workshop-rapportene (2007 og 2016) viser at MG-dysfunksjon er hovedårsaken til tårefordamping, som også er den vanligste årsaken til tørre øyne og ubehag på øyeoverflaten. Det er flere instrumenter tilgjengelig i markedet for MG-observasjon, diagnose og oppfølging. Infrarød lysteknologi er den vanligste, både innen forskning og klinisk praksis, etterfulgt av in-vivo konfokalmikroskopi og fremre segment OCT.

Målet med denne oversiktsartikkelen er å kondensere de nyeste bevisene innen MG-avbildning gjennom en narrativ oversikt over de mest brukte teknologiene inkludert andre nyere aspekter som kan bidra til å veilede klinikere og forskere innen øyeoverflaten og tørre øyne.

Nøkkelord: Meibomske kjertler (MG), MG-dysfunksjon, tørre øyne, diagnostisk avbildning, meibografi

Visualizzare il tarso palpebrale: una mini revisione

Riassunto

La visualizzazione del tarso palpebrale e delle ghiandole di meibomio (GdM) offre nuove opportunità per i professionisti della visione che lavorano nel campo della superficie oculare e dell'occhio secco a livello mondiale.

Il ruolo secretorio delle GdM gioca una parte fondamentale nel proteggere l'idratazione della parte anteriore della superficie dell'occhio creando uno scudo attivo composto di *meibum* (lipide) il quale riduce l'evaporazione e l'occhio secco. Evidenze dal popolare Dry Eye Workshop reports (2007 e 2016) dimostrano che la disfunzione delle GdM è la prima causa dell'occhio secco evaporativo la quale rappresenta la causa piu comune di occhio secco e discomfort della superficie oculare.

Una pletora di strumenti per l'osservazione, diagnosi e follow-up delle GdM sono disponibili nel mercato. Sembrerebbe che la tecnologie a luce infrarossa è la più comune in ricerca e nella pratica clinica grazie al suo anticipato sviluppo all'inizio degli anni 2000, seguita dalla microscopia confocale in-vivo e dall'OCT del segmento anteriore.

Ciònonostante, nuove tecnologie sono state messe a disposizione le quali potrebbero superare limiti quali costi e disponibilità delle stesse. L'obiettivo di questa mini-revisione è di condensare le ultime evidenze nel campo della visualizzazione delle GdM grazie ad una panoramica narrativa delle più comuni tecnologie considerando anche altri innovativi aspetti i quali potrebbero guidare clinici e ricercatori nel campo della superficie oculare e dell'occhio secco.

Parole chiave: Ghiandole di meibomio, disfunzione delle ghiandole di meibomio, occhio secco, diagnostica per immagini, meibografia.